Comparison of Three Algorithms for Filtering Airborne Lidar Data

Keqi Zhang and Dean Whitman

Abstract

This paper compares three methods for removing non-ground measurements from airborne laser scanning data. These methods, including the elevation threshold with expanding window (ETEW), maximum local slope (MLS), and progressive morphological (PM) filters, analyze data points based on variations of local slope, and elevation. Low and high-relief data sets with various densities of trees, houses, and sand dunes were selected to test the filtering methods. The results show that all three methods can effectively remove most non-ground points in both low-relief urban and high-relief forested areas. The PM filter generated the best result in coastal barrier island areas, whereas the other algorithms tended to remove the tops of steep sand dunes. Each method experienced various omission or commission errors, depending on the filtering parameters. Topographic slope is the most sensitive parameter for the three filtering methods.

Introduction

High-resolution digital terrain models (DTMs) are essential to model alluvial and coastal flooding, estimate erosion and accretion of land surfaces, and monitor landslides. Recent advances in airborne lidar (light detection and ranging) technology allow rapid and inexpensive measurements of topography over large areas. This technology is becoming the primary method to acquire high-resolution elevation data of ground objects. Airborne lidar systems record three-dimensional point measurements (*x, y*, and *z*) of objects scanned by the laser beneath the aircraft. These objects include both ground and non-ground features. Since a DTM is generated by interpolating the lidar measurements for the terrain, measurements from non-ground features such as buildings, trees, and vehicles have to be removed from a lidar data set before interpolation. The process of separating non-ground points from terrain measurements is referred to as "terrain filtering" and is a challenging research task in airborne lidar mapping applications.

A considerable number of algorithms have been created to filter lidar data. Okagawa (2001) used the cluster analysis technique to separate ground and non-ground lidar measurements. Kraus and Pfeifer (1998) filtered lidar data for forest areas using an iterative, linear least squares interpolation method. Pfeifer *et al.* (2001) expanded this method for lidar measurements in urban areas. Jacobsen and Passini (2001) and Passini and Jacobsen (2002) developed a filter based on linear prediction of stationary random function. Haugerud and Harding (2001) employed an algorithm to remove trees in forest areas by comparing local curvatures of point measurements. Vosselman (2000) proposed a filter to remove non-ground measurements by comparing slopes between a lidar point and its neighbors. The extension of the slope-based filter can be found in Roggero (2001) and Sithole (2001). Kilian *et al.* (1996), Lohmann *et al.* (2000), and Zhang *et al.* (2003) used mathematical morphology to identify non-ground measurements. Elmqvist (2001; 2002) classified ground and non-ground measurements based on active contours. Alternatively, lidar data can be filtered by selecting ground measurements iteratively from the original data set. Axelsson (2000) developed an adaptive Triangulated Irregular Network (TIN) method to find ground points based on selected seed ground measurements.

Relatively little work has compared various filtering methods in their accuracy, computation complexity, and sensitivity to filtering parameters despite the many algorithms that have been created. In addition, all published algorithms were applied to limited data sets. They have not been tested extensively for different earth surfaces such as vegetated mountains, building-dominated urban areas, and coastal barrier islands. The main objective of this paper is to present three filtering methods based on changes of local elevation and slopes, to compare these methods by applying them to various data sets from urban, coastal, and mountainous areas, and to test their sensitivity to various parameters used in the filtering process.

Terrain Filtering Methods

Elevation Threshold with Expanding Window (ETEW) Filter

Elevation differences between neighboring ground measurements are usually distinct from those between the ground and the tops of trees and buildings in an area of limited size. Therefore, elevation differences in a certain area can be used to separate ground and non-ground lidar measurements. The elevation threshold method uses an expanding search window to identify and remove non-ground points (Whitman *et al.*, 2003). First, the dataset is subdivided into an array of square cells, and all points, except the minimum elevation, are discarded. For the next iteration the cells are increased in size and the minimum elevation in each cell is determined. Then, all points with elevations greater than a threshold above the minimum are discarded. The process is repeated with the cells and thresholds increasing in size until no points from the previous iteration are discarded. For i^{th} iteration, a point $p_{i,j}$ is removed if

$$Z_{i,j} - Z_{i,\min} > h_{i,T} \quad (1)$$

Keqi Zhang of the Department of Environmental Studies and Dean Whitman of the Department of Earth Sciences are at the International Hurricane Research Center, Florida International University, Miami, FL 33199 (zhangk@fiu.edu; whitmand@fiu.edu).

Photogrammetric Engineering & Remote Sensing
Vol. 71, No. 3, March 2005, pp. 313–324.

0099-1112/05/7103–0313/$3.00/0

where $Z_{i,j}$ represents the elevation of j^{th} point ($p_{i,j}$) in a cell for i^{th} iteration, $Z_{i,min}$ is the minimum elevation in this cell, and $h_{i,T}$ is the height threshold. The $h_{i,T}$ is related to the cell size and defined by

$$h_{i,T} = sc_i \tag{2}$$

where s is a predefined maximum terrain slope, and c_i is the cell size for i^{th} iteration. In a simple implementation of this algorithm, the cell size c_i is doubled each iteration such that

$$c_i = 2c_{i-1} \qquad i = 2,3,\ldots M \tag{3}$$

where M is the total number of iterations.

The ETEW filter sometimes can create abrupt elevation changes of preserved ground measurements near cell boundaries because minimum elevations are different for each cell. To minimize this effect, the cell array is shifted by one half-cell size in the x and y directions and the filtering process is repeated for each iteration. Only points that satisfy the thresholds of the original and shifted cells are selected in each iteration.

Maximum Local Slope (MLS) Filter

Slopes of terrain are usually different from those between ground and the tops of trees and buildings. This slope difference can also be used to separate ground and non-ground measurements from a lidar data set. Vosselman (2000) developed a filter which identifies ground measurements by comparing local slopes between a lidar point and its neighbors. The method used in this paper is similar to Vosselman's filter. A lidar survey point, $p_0(x_0,y_0,z_0)$, is classified as a ground measurement if the maximum value ($s_{0,max}$) of slopes between this point and any other point (p_j) within a given radius is less than the predefined threshold (s):

$$\left\{ \begin{array}{c} s_{0,j} = \dfrac{z_0 - z_j}{\sqrt{(x_0 - x_j)^2 + (y_0 - y_j)^2}} \\ p_0 \in \textit{ground measurements} \quad \textit{if } s_{0,\max} < s \end{array} \right\} \tag{4}$$

where $s_{0,j}$ is the slope between p_0 and p_j, x_j and y_j represent the horizontal coordinates of p_j and z_j is its elevation.

Progressive Morphological Filter (PM)

Mathematical morphology uses operations based on set theory to extract features from images. This technology has been applied to filtering lidar data (Kilian *et al.*, 1996; Lohmann *et al.*, 2000). However, previous methods suffer various problems such as ineffective removal of various sized non-ground objects due to the requirement of a fixed window size.

Zhang *et al.* (2003) proposed an iterative PM filter to overcome these drawbacks. By gradually increasing the window size and using elevation difference thresholds, the PM filter removes measurements for different sized non-ground objects while preserving ground data. The procedure of the progressive morphological filter is listed as follows.

First, a rectangular mesh is overlain on the lidar data set. Each cell contains a point measurement $p_j(x_j, y_j, z_j)$ of the minimum elevation among the points whose coordinates fall within the cell. The cell size is usually selected to be smaller than the average spacing between lidar measurements so that most lidar points are preserved. If no measurements exist in a cell, it is assigned the value of its nearest neighbor. Elevations of points in the cells comprise an initial approximate surface.

In the second step, an opening (erosion + dilation) operation is performed on the initial surface to derive a secondary surface. The elevation difference ($dh_{i,j}$) of a cell j between the previous ($i-1$) and current (i) surfaces is compared to a threshold $dh_{i,T}$ to determine if the point p_j in this cell is a non-ground measurement. The threshold $dh_{i,T}$ is determined by

$$dh_{i,T} = \left\{ \begin{array}{cc} dh_0 & \textit{if } w_i \le 3 \\ s(w_i - w_{i-1})c + dh_0 & \textit{if } w_i > 3 \\ dh_{\max} & \textit{if } dh_{i,T} > dh_{\max} \end{array} \right\} \tag{5}$$

where dh_0 is the initial elevation difference threshold which approximates the error of lidar measurements (0.2–0.3 m), dh_{max} is the maximum elevation difference threshold, s is the predefined maximum terrain slope, c is the cell size of the mesh, and w_i is the filtering window size (in number of cells) at i^{th} iteration.

Third, the size of filtering window is increased and the derived surface model in the second step is used as the input for the opening operation. The second and third steps are repeated until the size of the filtering window is larger than the pre-defined maximum size of non-ground objects.

The maximum elevation difference threshold can be set either to a fixed value to ensure the removal of large and low buildings in an urban area or to the largest elevation difference in a study area. The filtering window can be a one-dimensional line or two-dimensional rectangle or any other shape. A line window was used in this paper. The opening operation was applied to both x and y directions at each step except for the coastal barrier island data set to ensure that the non-ground objects were removed.

Comparisons of Lidar Data Filters

Data Processing Before Filtering

In order to facilitate computation, all three filters were implemented using a two-dimensional array, whose elements represent points falling in cells of a mesh overlaying the data set. Each point measurement from the lidar data set is assigned into a cell in terms of its x and y coordinates. If more than one point falls in the same cell, one with the lowest elevation is selected as the array element. If no point exists in a cell, a no data indicator or interpolated point is assigned to corresponding array element, depending on the filtering method. After the array is generated, the filtering algorithms are performed on the points in the array.

Test Data Sets

Three data sets representing low-relief urban, coastal barrier island, and high-relief forested areas were used to test the filters. The urban data set is located at the campus of Florida International University (FIU), covering 1.6 km^2 of low relief areas (Figure 1). Surveyed features include residential houses, large buildings, single trees, forest stands, parking lots, open ground, ponds, roads, a major highway, and a canal. The data were collected in April 2000 with an Optech ALTM 1210 system operated by FIU. The data consist of three overlapping, 400 m wide swaths of 15 cm diameter footprints spaced approximately 2 m apart.

The coastal barrier island data set was collected by FIU on the south side of Cape Hatteras, North Carolina in June 2000. Features on the barrier island consist of beaches, sand dunes, and flat residential areas landward. The data consist of two overlapping, 300 m wide swaths of 13 cm diameter footprints spaced about approximately 1.6 m apart. About 3 km of surveyed barrier island were used in this study.

The data set for a forested area was downloaded from the Puget Sound Lidar Consortium (URL: http://www.pugetsoundlidar.org, last date accessed 20 December 2004) in Washington State. The features in this site are mainly high-relief terrain. Every flight covered a 600 m wide swath

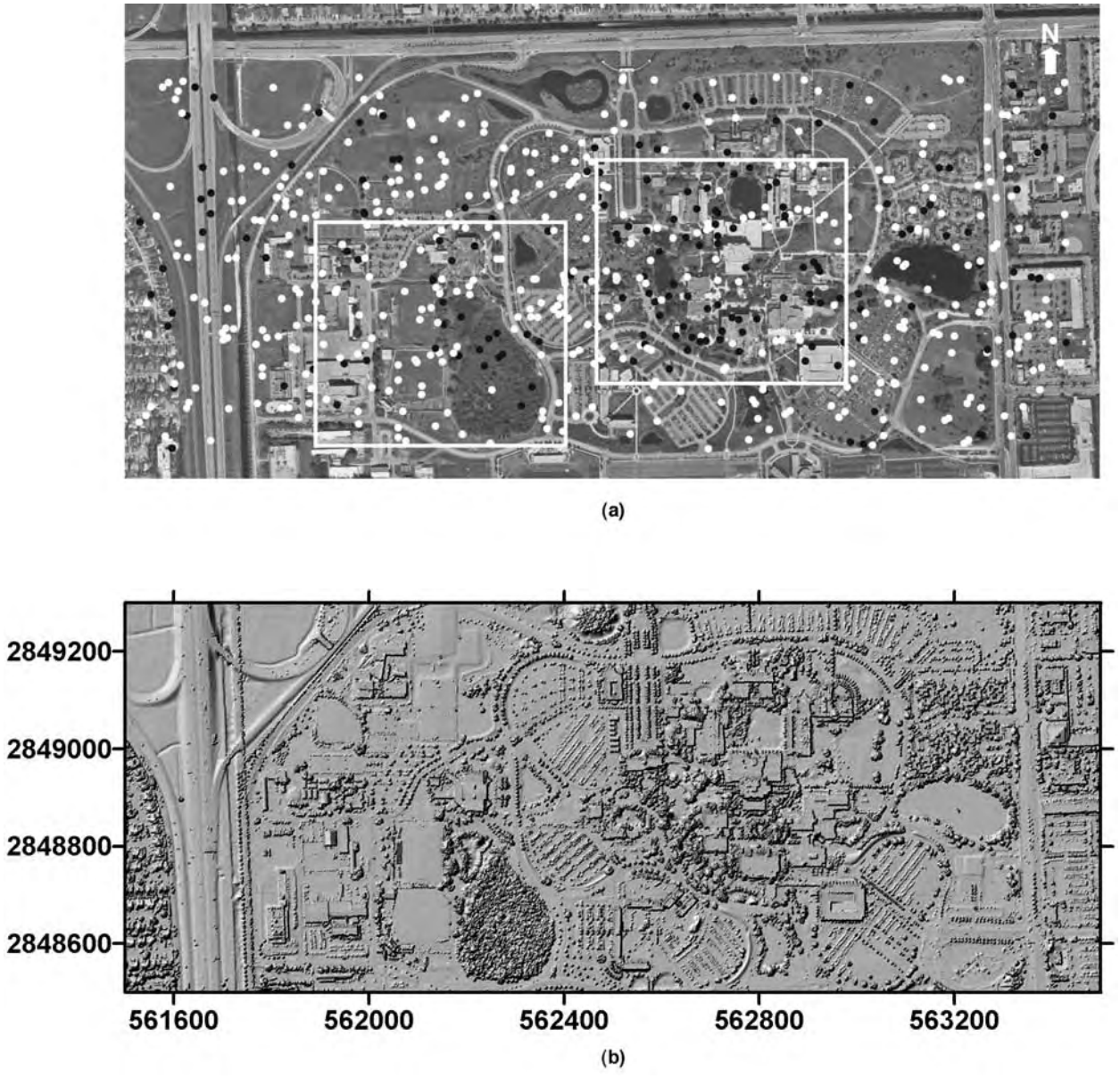

Figure 1. Low-relief urban test site: University Park campus of Florida International University. (a) Aerial photograph. 648 random sample points are also overlain over the photograph. The ground and non-ground measurements identified by the progressive morphological filter are represented by white and black dots, respectively. The rectangles represent the range of Figures 2 and 3. (b) Shaded relief map from unfiltered lidar measurements. Map coordinates (x and y) are in meters (UTM Zone 17).

with 0.9 m diameter laser footprints spaced at 1.5 m. The average density of one point per square meter was generated by setting up an overlap of more than half of the swath width between two adjacent flights.

Methods Used to Analyze Filtering Errors

There are two basic errors in filtering lidar data. One is to classify non-ground measurements as ground points, and the other is to select ground points as non-ground measurements. The former is called commission error, and the later is omission error (Congalton, 1991). All filtering methods are subject to these two errors in various degrees. To compare the effects of three filters, these errors have to be examined.

A straightforward idea would be to compare all filtered and unfiltered points to find omission and commission errors. However, this is impractical because millions of measurements are often involved in a single survey. An alternative way is to examine a sample of points selected at random. In this study, both qualitative and quantitative methods were employed to examine errors. The qualitative approach checked filtering errors by comparing the completeness of removing or preserving obvious features such as buildings and ponds. The quantitative method examined errors by comparing unfiltered and filtered measurements in a sample of test points selected at random.

Lidar measurements used in the quantitative error analysis were selected by the following process. First, a set of random x and y coordinates were selected within the bounds of the data set. Then, lidar measurements that fell within 1 m square cells containing the random coordinates

were selected as test points. Points classified as ground measurements by the filter were assigned a value of 1, while non-ground measurements were assigned a value of 0. Finally, the test points were overlain on aerial photographs in a GIS and classified visually as being ground or non-ground features. If necessary, features were verified in the field in order to avoid misinterpretation.

The quantitative error analysis was only performed on the FIU data set. It has not been applied to the Cape Hatteras and Puget Sound data sets because either field examination is cost-prohibitive or simultaneously collected aerial photographs for test areas are not available.

Results of Filter Tests

Low-relief Urban Area

Tables 1, 2, and 3 present the filtering parameters for the FIU campus data set. These "optimum" parameters were selected by examining topographic changes in the study area and comparing unfiltered and filtered results iteratively. A 2.5 m maximum elevation difference threshold for the PM filter was used to ensure the removal of building complexes. There are about one million lidar measurements for this area, and the number of mesh cells required to hold the data is about two million. Among them, 712,000 cells have data, and about 30 percent of points were removed as repeated measurements for each cell. About 68 percent, 70 percent, and 74 percent of points in cells having data were classified as ground measurements by ETEW, MLS, and PM filters, respectively.

TABLE 1. PARAMETERS FOR ETEW METHOD. UNITS ARE IN METERS

Location	FIU Campus	Hatteras Beach	Puget Sound
Initial Cell size (c_i in Equation 3)	1	1	1
Slope (s in Equation 2)	0.1	0.15	1
Number of Iteration (M in Equation 3)	7	6	5

TABLE 2. PARAMETERS FOR MLS METHOD. UNITS ARE IN METERS

Location	FIU Campus	Hatteras Beach	Puget Sound
Cell Size	1	1	1
Search Radius	45	20	10
Slope Threshold (s in Equation 4)	0.2	0.25	1

Figure 2 presents the grids from raw and filtered lidar measurements for a mostly building-free area of the FIU campus. Cars, buildings, individual trees, and a forest stand are dispersed over the flat terrain surface (Figure 2a). The filtered results show that most non-ground objects were removed by the three filters. However, various omission and commission errors were committed by the filters. For example, a small mound (**M** in Figure 2a) was removed completely by the ETWE and MLS filters (**O** in Figures 2b and 2c), while part of it passed the PM filter (**O** in Figures 2d).

Several tree measurements in a forest stand were not removed (commission error) by all three filters. The number of commission errors in the forest area is relatively small for the ETEW filter (**C** in Figure 2b). More commission errors were generated by MLS and PM filters (Figures 2c and 2d). Figure 3 shows unfiltered and filtered data for an area with many buildings at the FIU campus. The ETEW and PM method filtered out buildings well, while the MLS method did not remove the building completely (**C** in Figure 3c). Also, the ETEW and MLS filters generated omission errors in a small mound area (**O** in Figures 3b and 3c).

The three filters performed relatively well at the FIU site. However, there are some differences when they process certain features. For example, all three filters tend to remove small mounds. The MLS and ETEW methods committed more these types of errors than the PM filter (Figure 2). In contrast, all three filters preserve roads well.

MLS and ETEW algorithms tend to remove ground points surrounding relatively low measurements, leading to a distortion of the DTM. For example, boundaries of ponds were dilated by interpolation because of this omission error (**P** in Figures 4a and 4b). This dilation effect is illustrated more clearly around a low-lying drainage area (**B** in Figure 4). Neighbors of these low-elevation measurements are removed mistakenly. Interpolating the isolated low measurements generates an artificial feature, i.e., "bomb crater" (**B** in Figures 4a and 4b), a circular region of low elevation. The size of these features are minimized in the PM filter (Figure 4c).

Large buildings cannot be removed completely by the MLS filter if the search radius is less than half of the sizes of the buildings. We can minimize this error by excluding measurements outside a given range before filtering. In order to make this solution work, the range has to be higher than the terrain in the filtered area and lower than the roofs of large buildings. Obviously, this condition is more easily satisfied in low-relief urban areas than in high-relief areas. However, the range is sometimes hard to find even in the flat urban areas. The ETEW and PM filters do not have the above limitation. By increasing window size gradually, large buildings are removed as long as their heights are larger than the thresholds.

Quantitative error examination shows that commission and omission errors committed by the filters range from

TABLE 3. PARAMETERS FOR THE PM METHOD. UNITS ARE IN METERS

Location	FIU Campus	Hatteras Beach	Puget Sound
Cell Size (c in Equation 5)	1	1	1
Window Size (w_i in Equation 5)	3, 5, 9, 17, 33, 65, 129, 257, 513	3, 5, 9, 17, 33, 65, 129, 257, 513	3, 5, 9, 17, 33
Slope (s in Equation 5)	0.08	0.08	1.2
Initial Threshold (dh_0 in Equation 5)	0.25	0.2	0.1
Maximum Threshold (dh_{max} in Equation 5)	2.5	20*	210*
Rotate Angle (Anticlockwise, Degree)	0	69	0

*The maximum threshold was set to the largest elevation difference in the study area.

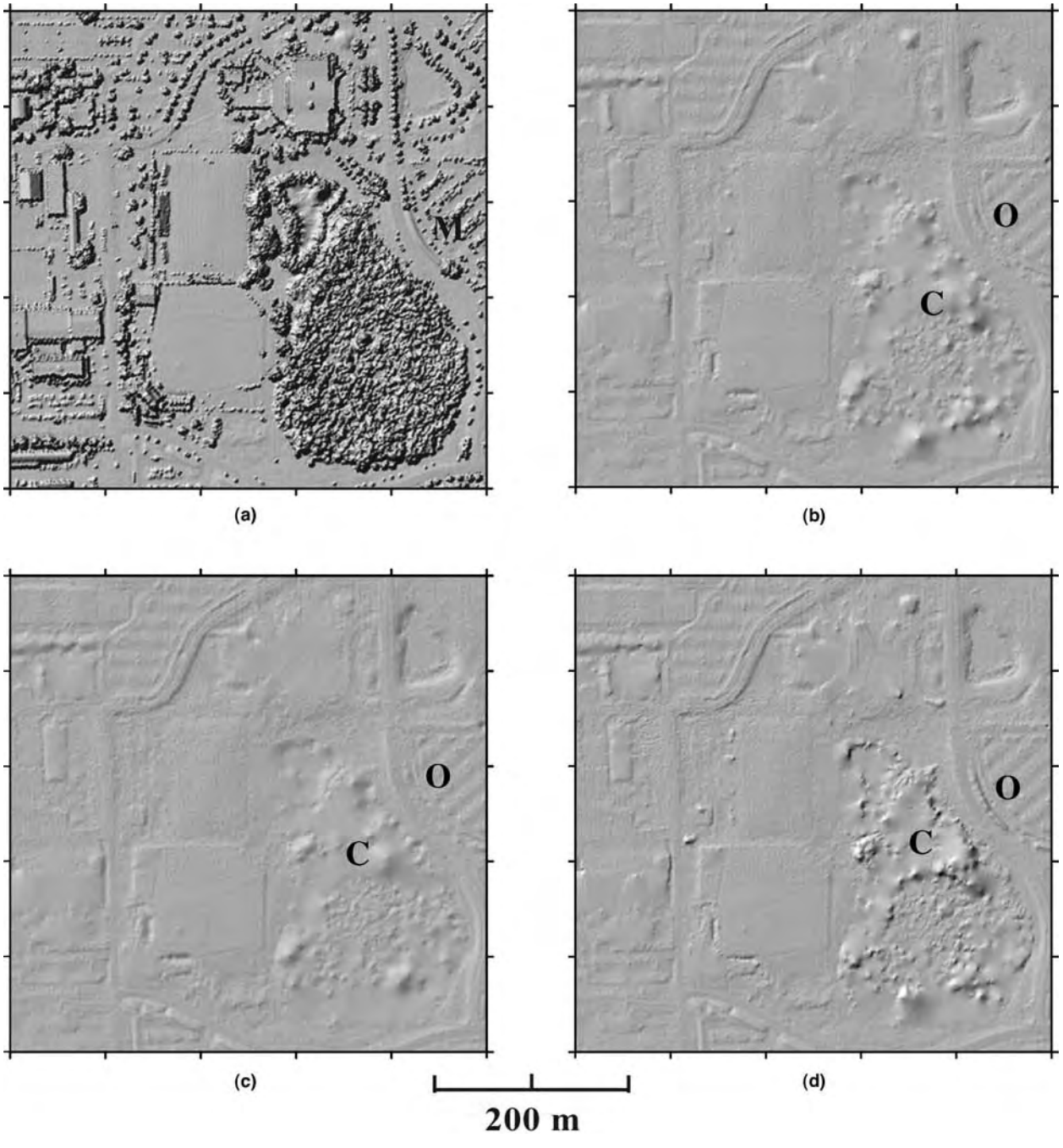

Figure 2. Comparison of filtering methods at a region of the FIU campus containing mostly vegetation and athletic fields. Shaded relief maps for the DTMs generated from (a) unfiltered lidar data, (b) the ETEW filter, (c) the MLS filter, and (d) the PM filter. The data were interpolated to a 1 m resolution grid using the method of a Kriging with a 100 m search radius. Most nonground measurements were removed successfully by filters. However, a few measurements for tree (**C**) remained because of high tree density and a small mound was mistakenly removed (**O**). **C** refers to commission errors; **O** refers to omission errors.

3 percent to 7 percent of total samples (Table 4), indicating that all three filters worked well at low-relief urban areas. The PM filter committed less errors than ETEW and MLS methods. One reason for having more errors by the ETEW filter is that this algorithm tends to generate a more sparse set of ground measurements. It should be pointed out that the sparseness of these points does not necessarily lead to a worse DTM interpolation. The effects of the error distribution in space on DTM generation needs further study.

Low-relief Coastal Barrier Island

The second data set comes from a barrier island coast on the south side of Cape Hatteras in North Carolina (Figure 5a). The U.S. East and Gulf Coasts are dominated by barrier islands. Sand dunes, a common landform at barrier coasts, often have a long and elevated shape. The sand dunes are buffers to reduce the impact of coastal storms to property behind the dunes. Their effects are mainly determined by their size and shape. Therefore, it is important to accurately

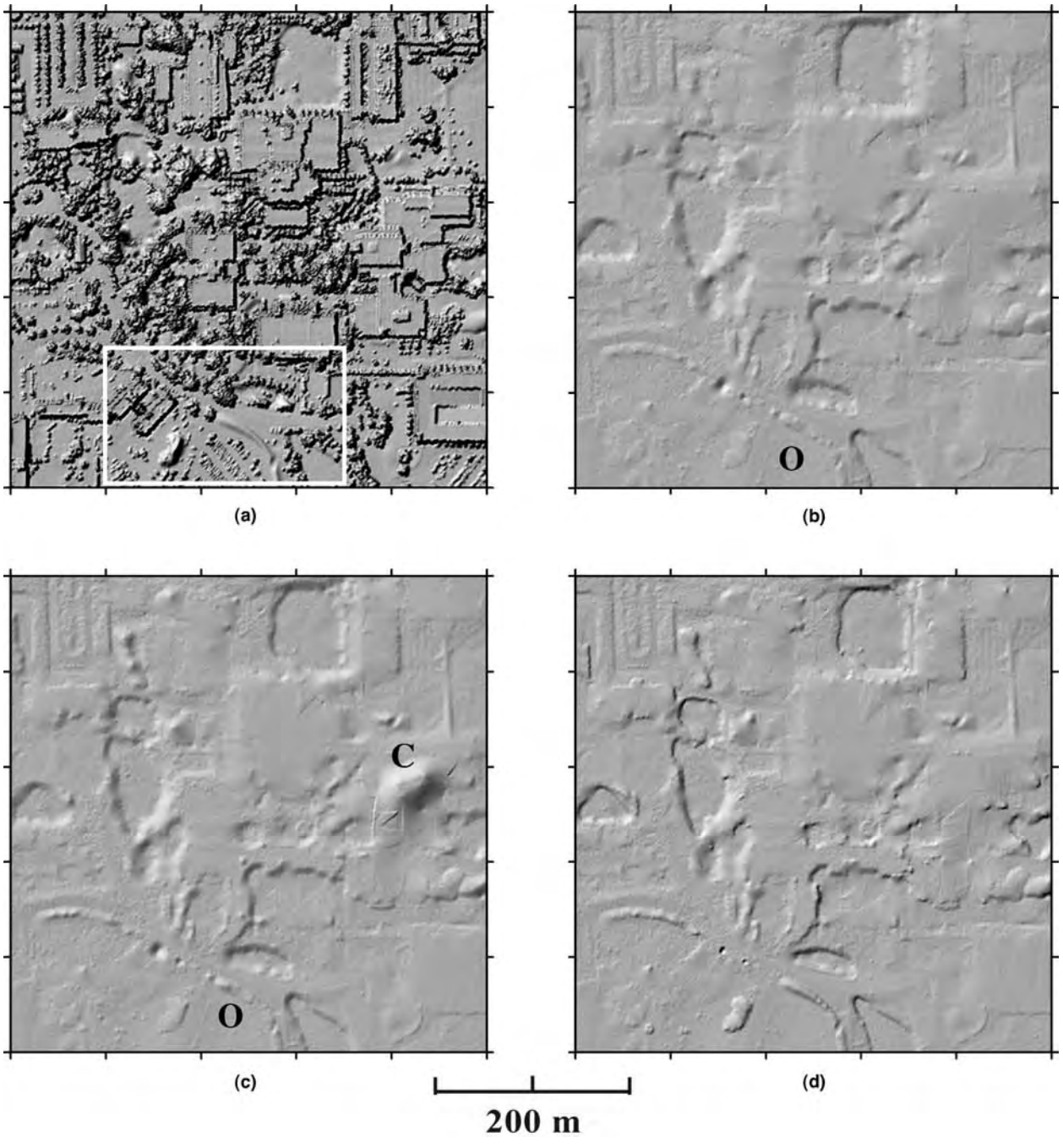

Figure 3. Shaded relief maps for raw and filtered data from a built up area at the FIU campus. (a) Raw lidar measurements, (b) the ETEW filter, (c) the MLS filter, and (d) the PM filter. The box in (a) indicates the area shown in Figure 4.

extract geometric information of sand dunes from lidar measurements. Since their shapes are similar to that of a line of trees or buildings (Figure 6), sand dunes are often removed by filtering algorithms.

Examples of this "over filtering" are shown in Figures 5b and 5c. Both the ETEW and MLS filters tend to remove the tops of the dunes. This occurs because while small slope thresholds are required to remove features such as buildings and cars from areas behind the dunes, the natural slope on the backside of the dune can be quite high, often exceeding 1:4 (Figure 6).

Fortunately, the shorelines of most barrier coasts are usually smooth, and the ridges of dunes are parallel to the shoreline. The straight, long, and elevated shape of a sand dune allows itself to be identified by the PM filter. However, some data preprocessing is required to make the PM filter work. The PM filter removes features with steep slopes within a window. If the opening operation is performed along the direction perpendicular to the shoreline, the top of a sand dune will be removed. This problem can be solved by rotating an overlain mesh so that it is parallel to ridges of the sand dunes. Then, an opening operation is performed

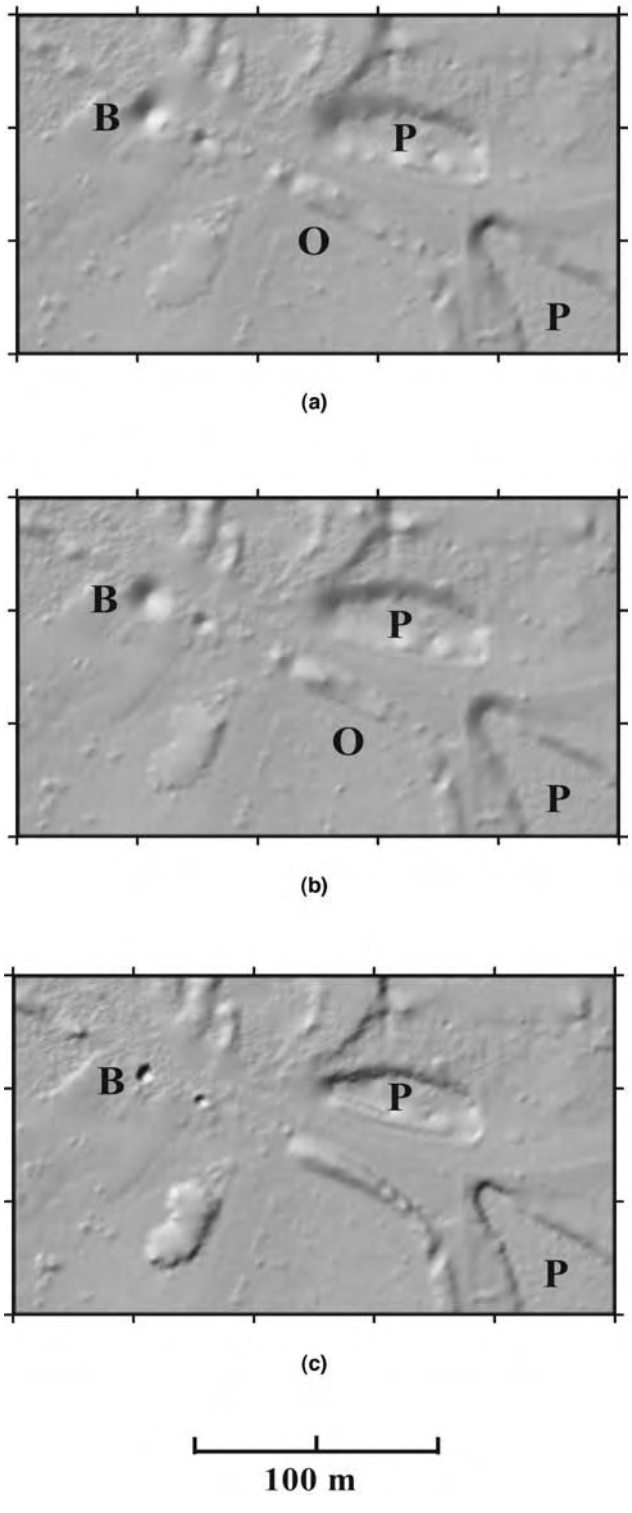

Figure 4. Effect of anomalous low elevation measurements on a DTM. Note that a "bomb crater" (**B** as shown in a and b) caused by the isolated low-elevation measurements of the underground drainage system because of filtering errors from ETEW (a) and MLS (b) methods. The boundary of ponds (**P** as shown in a and b) were also dilated by these two methods. The boundaries of the low elevation measurements and ponds were well preserved by the PM filter (c).

TABLE 4. NUMBER OF ERRORS COMMITTED BY THREE FILTERS IN A RANDOM SAMPLE

Filtering Method	Number of samples	Number of comission errors	Number of commission errors	Percentage of all errors
ETEW	648	48	0	7
MLS	648	46	2	7
PM	648	17	2	3

along either the rotated *x* or *y* direction using a line window. The sand dunes will not be removed in this way because the size of a sand dune is larger than those of line filtering windows.

The measurements for the barrier island at Cape Hatteras were rotated anticlockwise with an angle of 69 degrees before filtering to align the ridges of sand dunes to the *x* direction. Then, an opening operation along the *x* direction was applied to the data set. The filter parameters are listed in Table 3. The maximum elevation difference threshold was set to the largest elevation difference in the study area to preserve sand dunes. Figure 6 demonstrates that sand dunes and beaches are well preserved by the PM filter, while the buildings and trees are removed.

High-relief Forested Area

For the high-relief topographic data set at Puget Sound, Washington, there are about 2.68 million raw lidar measurements, and the number of grid cells to hold the data is 1.4 million. Among them, 0.91 million cells have data, and about 76 percent of the points were removed as repeated measurements for each cell because this data set includes multi-returns of the same laser pulse. About 62 percent, 53 percent, and 49 percent of points in cells having data were classified as ground measurements by the ETEW, MLS, and PM filters, respectively.

Good results were achieved by applying three filters to this data set as shown in Figure 7. The valleys and ridges that are not obvious in the digital surface model created from unfiltered data (Figure 7a) are clearly shown in the DTMs from the filtered data (Figures 7b, c, and d). However, some low vegetation has not been removed completely as indicated by mottled areas in the filtered shaded relief maps. The MLS filter is the most effective in removing these features.

As in the low-relief test areas, the ETEW and MLS filters often generate "bomb craters," resulted from interpolation of isolated low measurements. Examples are shown in Figures 7b and 7c. In contrast, the PM filter is less susceptible to this type of artifact because it preserves the boundary of low-elevation measurements (**B** in Figure 7d).

Sensitivity Analysis

The filtering results are determined by input parameters such as thresholds (Equations 2, 4, and 5), the cell size of the mesh grid (*c* in Equations 2 and 5), and density of point measurements. The common factor that influences threshold values for the three filters studied here is the maximum slope (*s* in Equations 2, 4, and 5). Testing shows that the slope is the most sensitive parameter for all three methods. Currently, optimum slope is selected by examining the topographic changes of the study area and comparing unfiltered and filtered results iteratively. The development of an objective method such as one based on slope distribution to determine optimum slope parameter needs to be further investigated.

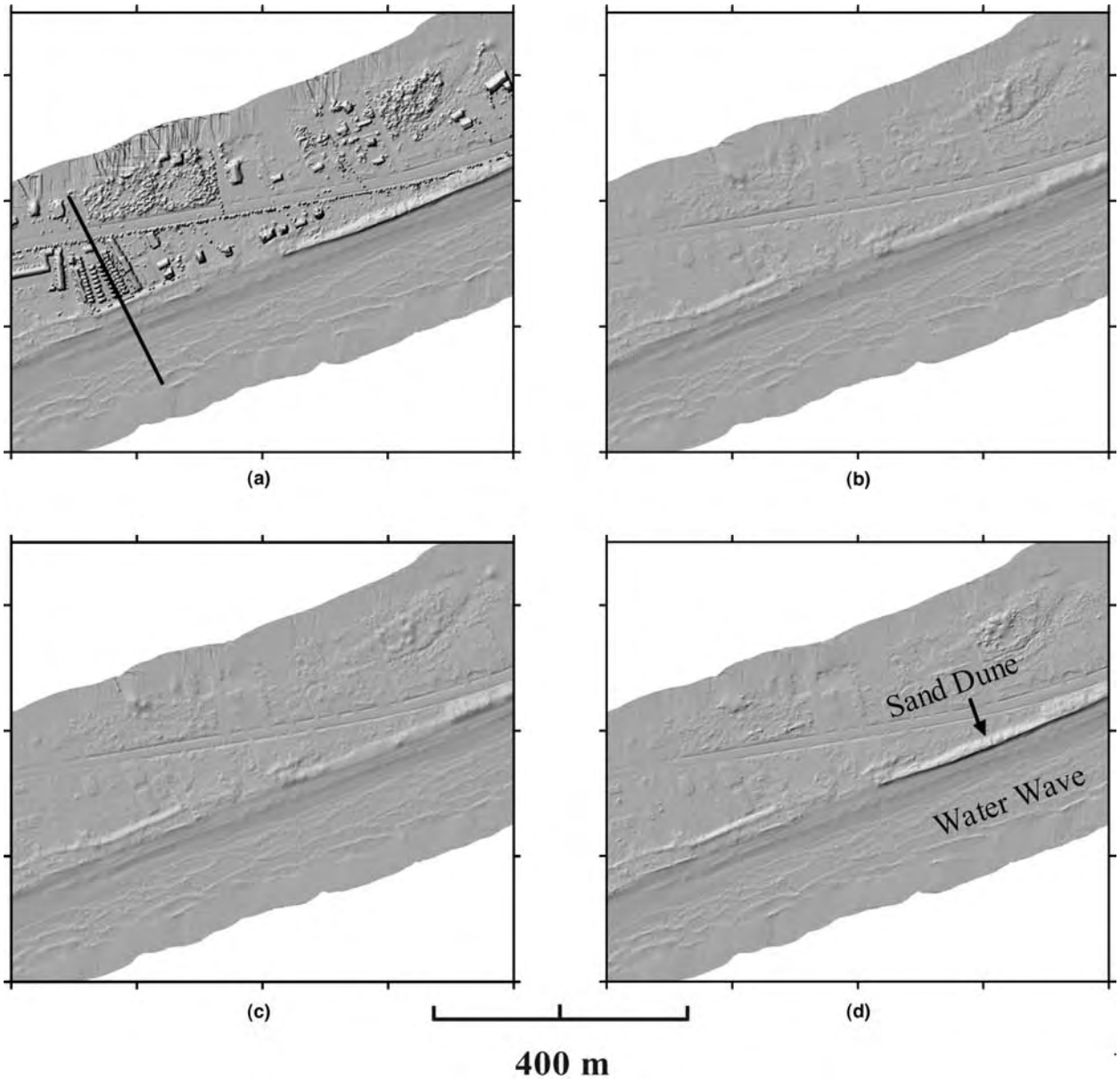

Figure 5. Shaded relief maps comparing filtering methods at Cape Hatteras in North Carolina. (a) Unfiltered lidar data, (b) the ETEW filter, (c) the MLS filter, and (d) the PM filter. The data were interpolated to a 1 m resolution grid using the method of Kriging with a 50 m search radius. Note that ETEW and MLS methods removed the tops of sand dunes mistakenly, while the PM method preserved them. The solid line in (a) indicates the location of the profile in Figure 6.

To examine the effect of point density, the original lidar measurements from the FIU data set were resampled first using cell size 2 m × 2 m, 3 m × 3 m, 4 m × 4 m, 5 m × 5 m, and 6 m × 6 m. For each cell, the point closest to the center of the cell is selected when resampling is performed. Then, each filtering method was applied to the resampled data.

The parameters listed in the Tables 1, 2 and 3 were used for filtering the resampled data sets. The effect of point density is most remarkable between filtered grids from the original and 6 m × 6 m resampled data sets (Figure 8). The 6 m × 6 m resolution data generated a less detailed DTM than that from the full resolution data. The small mounds and boundaries of ponds (**P** in Figure 8) were obscured in the DTMs from low-resolution data. The large objects such as individual trees and buildings were removed in both the original and 6 m × 6 m resolution data. However, residuals of small objects such as cars in the parking lot become evident in the DTMs from low-resolution data, especially those interpolated using the data from MLS and ETEW filters. There are two reasons for this phenomenon. One is that low-resolution data are more susceptible to commission errors. The other is that these commission errors in low-resolution data sets have more effect on DTMs than those in high-resolution data sets. The effect of commission errors from high-resolution data on a DTM is limited because they are surrounded closely by ground points (Figures 8b, 8d, and 8f). Resampling schemes of 2 m × 2 m, 3 m × 3 m, 4 m × 4 m, and 5 m × 5 m have the same effect of that of 6 m × 6 m, but less notable.

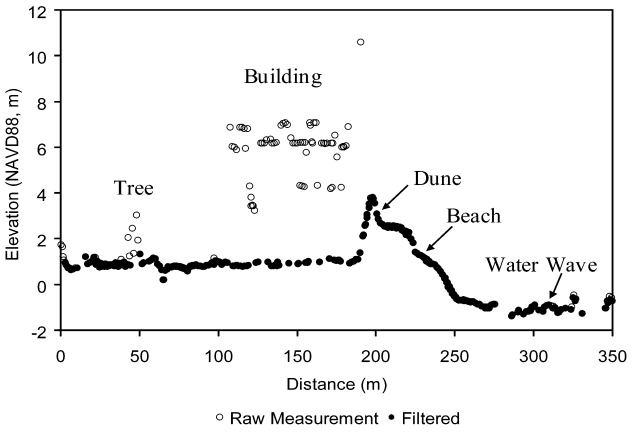

Figure 6. Unfiltered and filtered (PM filter) lidar measurements along a transect at Cape Hatteras. Points were projected onto the line of section over a 1.5 m wide swath. Tree and house objects are removed successfully by the progressive morphological filter, while the measurements for the sand dune and beach are preserved.

The influence of the mesh cell size (c in Equations 2 and 5) on filtering results is similar to that of the point data density, because all three filters are implemented by an array which involves resampling data for mesh cells in terms of x and y coordinates and vertical elevations of raw measurements.

Time Complexity of Computation

The computation time for a filtering method is determined by filtering parameters and implementation. For the array implementation used in this study, the time complexity of the ETEW filter is

$$O(\sum_{i=1}^{M} n_i) \leq O(MN) \tag{6}$$

where N is the total number of cells in the mesh generated in terms of x and y coordinates of raw lidar measurements as previously discussed. M is the number of iterations, n_i is the number of points preserved by the filter in i^{th} iteration, n_1 is equal to N, and $n_i \leq N$. For the MLS with a search radius of r, the time complexity in an array implementation can be represented by

$$O(r^2 N) \tag{7}$$

where r is measured by the number of cells. The computation time of the PM filter consists of two parts: nearest neighbor interpolation and opening operation. Assuming that the average search radius ($\bar{r}$) is needed to find a nearest neighbor, the time complexity approximates to

$$O(\bar{r}^2 N + \sum_{i=1}^{M} w_i N) \tag{8}$$

where w_i is the size (number of cells) of the i^{th} window and M is the number of windows used by the filter.

Comparison of Equations 6, 7, and 8 indicates that the ETEW filter usually requires the least amount of computation time. Progressive PM filter takes a moderate amount of time because $\bar{r}$ is usually small. The MLS filter needs the longest amount of time because the computation time increases quickly as the search radius enlarges. For an array of 2 million elements used in the FIU campus data set, the computation time was 22, 78, and 500 seconds for the elevation threshold with ETEW, PM, and MLS filters, respectively. The parameters in Tables 1, 2, and 3 were used by the filters, and all algorithms were implemented in the C++ environment. The machine used to perform the computation was a Microsoft Windows® 2000 workstation with 2 GB RAM and a 2.2 GHZ Pentium 4 processor.

Conclusions

For a low-relief urban data set all three filtering methods worked well. However, none of them worked perfectly, and all methods are susceptible to both omission and commission errors. Quantitative error analysis shows that the PM filter committed the least errors, and the ETEW and MLS filters produced more errors. For the coastal barrier island, the PM filter achieved the best result. In high-relief areas, all three filters generated satisfactory results. The MLS filter is most effective in removing low vegetation.

The PM filter is very effective in preserving features and their boundaries that are larger than the filtering window size. This capacity is very useful in extracting the three-dimensional character of some geomorphic forms such as coastal sand dunes and cliffs. The ETEW and MLS methods tend to dilate the boundaries of areas with lower elevation relative to their neighbors. All three methods are most sensitive to the slope parameters in the thresholds. Lidar data point density has relatively less effect on the filtering results, but does have an impact on digital surface or terrain models, depending upon the resolution of the data set and changes of topography in a study area.

The ETEW method is the fastest filter, while the MLS method is the slowest. The PM filter needs a moderate amount of computation time. Numerical experiments show that computation time of current array implementation for the three filters is acceptable and can be performed on low-cost personal computers.

Acknowledgments

This research was partly supported by a grant from Federal Emergency Management Agency.

References

Axelsson, P., 2000. DEM generation from laser scanner data using adaptive tin models, *International Archives of Photogrammetry and Remote Sensing*, XXXIII, Part B3:85–92.

Congalton, R.G., 1991. A review of assessing the accuracy of classifications of remotely sensed data, *Remote Sensing of Environment*, 37(1):35–46.

Elmqvist, M., 2002. Ground surface estimation from airborne laser scanner data using active shape models, *ISPRS Commission III Symposium, Photogrammetric and Computer Vision*, Graz, Austria, pp. 114–109.

Elmqvist, M., E. Jungert, F. Lantz, A. Persson, and U. Soderman, 2001. Terrain modelling and analysis using laser scanner data, *International Archives of Photogrammetry and Remote Sensing, XXXIV*, Part 3/W4:219–226.

Haugerud, R.A., and D.J. Harding, 2001. Some algorithms for virtual deforestation (VDF) of LIDAR topographic survey data, *International Archives of Photogrammetry and Remote Sensing*, XXXIV, Part 3/W4:211–218.

Jacobsen, B.D., and R. Passini, 2001. Filtering of digital elevation models, GIS 2001, 19–22 February, Vancouver, 8 p., unpaginated CD-ROM.

Kilian, J., N. Haala, and M. Englich, 1996. Capture and evaluation of airborne laser scanner data, *International Archives of Photogrammetry and Remote Sensing*, XXXI, Part B3:383–388.

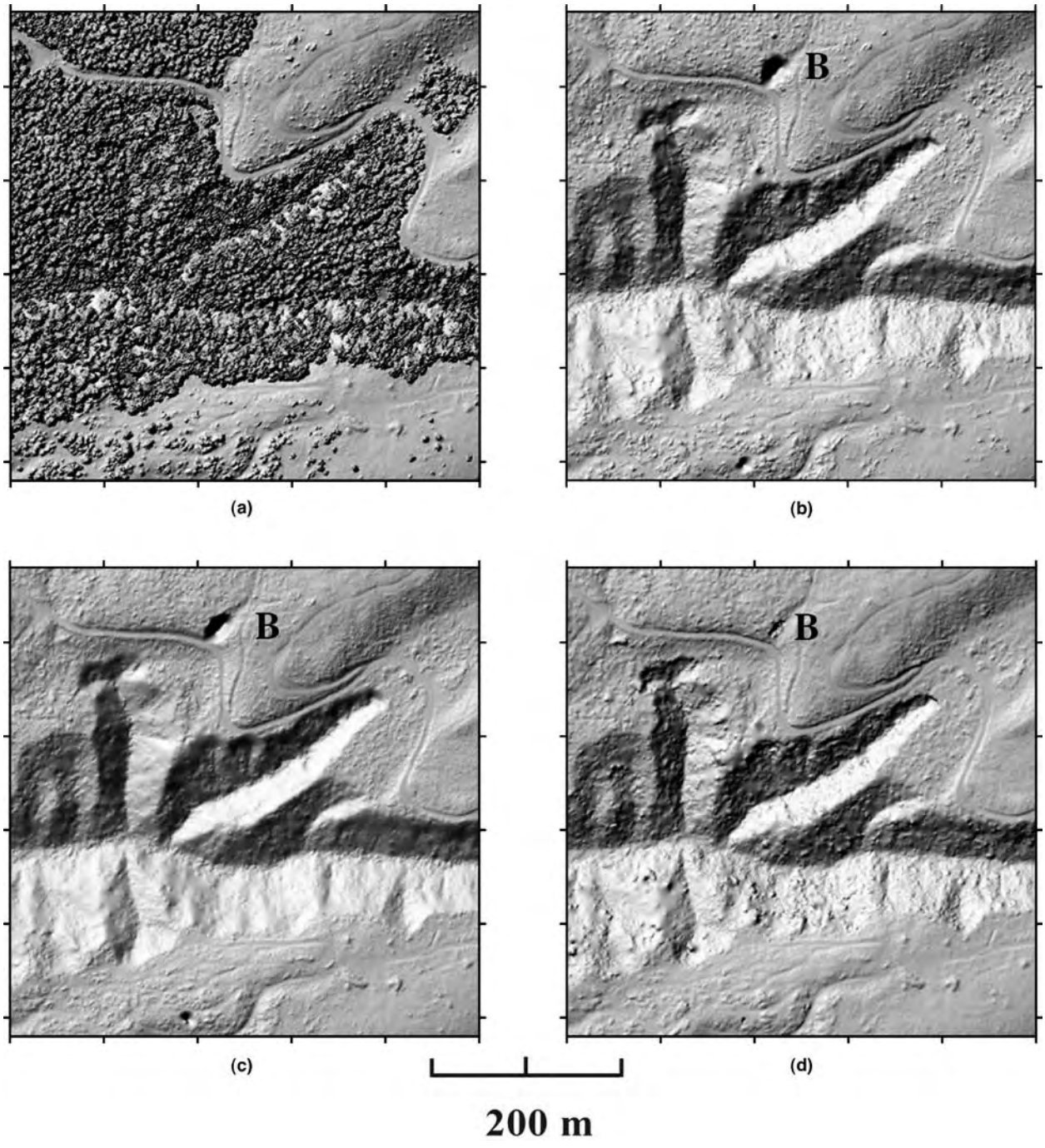

Figure 7. Shaded relief maps comparing filtering methods at Puget Sound, WA. (a) Unfiltered lidar data, (b) the ETEW filter, (c) the MLS filter, and (d) the PM filter. The data were interpolated to a 1 m resolution grid using the method of Kriging with a 50 m search radius. The topography of valleys is clear, and linear features such as roads are well preserved in the filtered images. The MLS filter generated the smoothest image. A "bomb crater" generated by a pit at the top of the mountain was obvious in images from ETEW and MLS filters (**B** as shown in b and c).

Kraus, K., and N. Pfeifer, 1998. Determination of terrain models in wood areas with airborne laser scanner data, *ISPRS Journal of Photogrammetry & Remote Sensing*, 53(4):193–203.

Lohmann, P., A. Koch, and M. Schaeffer, 2000. Approaches to the filtering of laser scanner data, *International Archives of Photogrammetry and Remote Sensing*, XXXIII, Part B3:540–547.

Okagawa, M., 2001. Algorithm of multiple filter to extract DSM from LIDAR data, *2001 ESRI International User Conference*, ESRI, San Diego, California (URL: http://www.esri.com, last date accessed 20 December 2004).

Passini, R., and B.D. Jacobsen, 2002. Filtering of digital elevation models, *Proceedings of the ASPRS 2002 Annual Convention*, 19–26 April, Washington DC (American Society for Photogrammetry and Remote Sensing, Bethesda, Maryland), 9 p., unpaginated CD-ROM.

Pfeifer, N., P. Stadler, and C. Briese, 2001. Derivation of digital terrain models in the SCOP++ environment, *Proceedings of*

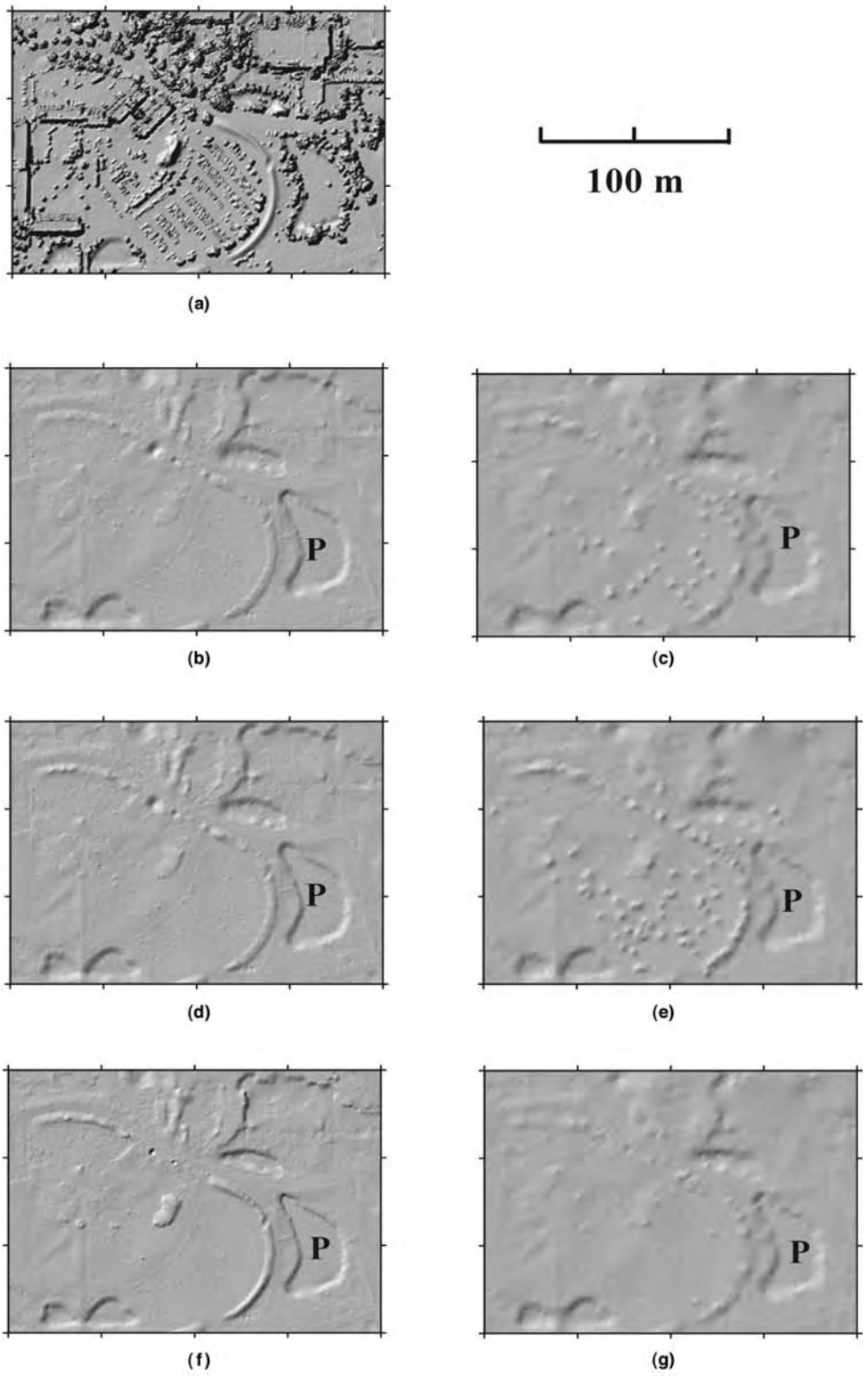

Figure 8. DTMs show sensitivity of filters to point measurement density. (a) Unfiltered lidar measurements, (b) the ETEW filter for original measurements, (c) the ETEW filter for 6 m × 6 m resampled data, (d) the MLS filter for original measurements, (e) the MLS filter for 6 m × 6 m resampled data, (f) the PM filter for original measurements, and (g) the PM filter for 6 m × 6 m resampled data. In comparison with DTMs from original data sets, those from 6 m × 6 m data sets lose details and boundaries of ponds are blurred, which is mainly caused by low data density.

OEEPE Workshop on Airborne Laserscanning and Interferometric SAR for Detailed Digital Elevation Models, 01–03 March 2001, Stockholm, Sweden, 13 p.

Roggero, M., 2001. Airborne laser scanning: clustering in raw data, *International Archives of Photogrammetry and Remote Sensing*, XXXIV, Part 3/W4:227–232.

Sithole, G., 2001. Filtering of laser altimetry data using a lope adaptive filter, *International Archives of Photogrammetry and Remote Sensing*, XXXIV, Part 3/W4:203–210.

Vosselman, G., 2000. Slope based filtering of laser altimetry data, *International Archives of Photogrammetry and Remote Sensing*, XXXIII, Part B4:958–964.

Whitman, D., K. Zhang, S.P. Leatherman, and W. Robertson, 2003. Airborne laser topographic mapping: application to hurricane storm surge hazards, *Earth Sciences in the Cities* (G. Heiken, R. Fakundiny, and J. Sutter, editors), American Geophysical Union, Washington DC, pp. 363–376.

Zhang, K., S. Chen, D. Whitman, M. Shyu, J. Yan, and C. Zhang, 2003. A progressive morphological filter for removing non-ground measurements from airborne LIDAR data, *IEEE Transactions on Geoscience and Remote Sensing*, 41(4):872–882.

(Received 23 June 2003; accepted 08 December 2003; revised 13 January 2004)

Call for Papers

The 20th Biennial Workshop on Aerial Photography, Videography, and High Resolution Digital Imagery for Resource Assessment

October 4-6, 2005 — Weslaco, Texas, USA

Sponsored by

American Society for Photogrammetry and Remote Sensing

Hosted by

USDA-ARS Kika de la Garza Subtropical Agricultural Research Center

Workshop Co-Chairs

James H. Everitt and Chenghai Yang

This workshop seeks papers on applications of photography, videography, and high-resolution multi-spectral and hyperspectral imagery for monitoring and managing agricultural and natural resources. Papers on new imaging systems and innovative applications of GIS and image processing and analysis techniques are also solicited. A special session on remote sensing applications in precision agriculture is planned.

Of particular interest are papers using

- Field spectroradiometers
- Aerial multispectral videography
- High resolution satellite imagery (IKONOS, QuickBird, & SPOT)
- GIS
- Color and color-infrared aerial photography
- Airborne multispectral and hyperspectral imaging systems
- Multispectral and hyperspectral image analysis techniques

For applications in

- Forestry
- Riparian and wetland areas
- Water quality
- Precision agriculture
- Wildlife, urban, and other resources
- Rangelands
- In-stream fisheries habitats
- Agricultural land and crops
- Pest management

Abstract Submission

Authors are invited to submit abstracts with approximately 250 words by **June 1, 2005**. Full papers are due before or during the workshop. A conference proceedings will be published on a CD-ROM shortly after the workshop.

All abstracts should be submitted electronically to James Everitt at jeveritt@weslaco.ars.usda.gov or to Chenghai Yang at cyang@weslaco.ars.usda.gov. If regular mail has to be used, please include a hardcopy and an electronic copy of the abstract to:

James H. Everitt or Chenghai Yang
USDA-ARS, Kika de la Garza Subtropical Agricultural Research Center, Weslaco, Texas 78596 USA
Tel: 956-969-4812 or 4824; Fax: 956-969-4893

Important Due Dates

Abstract submission — June 1, 2005
Acceptance notification — July 1, 2005
Full paper submission — October 4, 2005

Weslaco is located at the south tip of Texas, only 7 miles from Mexico and 60 miles from the Gulf of Mexico. The Texas A&M University's Texas Agricultural Experiment Station is adjacent to the USDA-ARS Weslaco Research Center.